High-speed wide-field time-gated endoscopic fluorescence-lifetime imaging

J. Requejo-Isidro, J. McGinty, I. Munro, D. S. Elson, N. P. Galletly, M. J. Lever, M. A. A. Neil, G. W. H. Stamp, and P. M. W. French

Department of Physics, Division of Investigative Sciences and Department of Bioengineering, Imperial College London, London SW7 2AZ, UK

P. A. Kellett, J. D. Hares, and A. K. L. Dymoke-Bradshaw

Kentech Instruments, Ltd., Unit 9, Hall Farm Workshops, South Moreton, Didcot, Oxon OX11 9AG, UK

Received April 23, 2004

We report the development of a high-speed wide-field fluorescence-lifetime imaging (FLIM) system that provides fluorescence-lifetime images at rates of as many as 29 frames/s. A FLIM multiwell plate reader and a potentially portable FLIM endoscopic system operating at 355-nm excitation have been demonstrated.

OCIS codes: 170.3650, 170.3880, 170.2150, 170.6920, 170.6280.

Imaging autofluorescence offers the potential for minimally invasive diagnosis of disease, e.g., for the detection of precancerous lesions in the uterine cervix.[1] Fluorescence endoscopy may permit *in vivo* real-time imaging of variations in chemical and physical parameters of biological tissue and so reduce the need for conventional (invasive) techniques such as excision biopsy and cytology. Fluorescence-lifetime imaging (FLIM) is particularly interesting because it can provide biochemical[2] and structural information derived from tissue autofluorescence to yield intrinsic contrast.[3] FLIM is also relatively robust against variations in fluorophore concentration or excitation intensity (caused by uneven illumination or intervening absorption or scattering) and against nonuniform fluorescence collection efficiency.

FLIM entails determining the fluorescence decay characteristics at each spatially resolvable location within a fluorescence image and may be implemented in almost any optical instrument including microscopes, endoscopes, and multiwell plate readers. One can measure the fluorescence lifetime in the frequency domain by measuring the phase shift or modulation in a fluorescence signal obtained by excitation of the sample with, e.g., either a pulsed or a high-frequency modulated source.[4] Alternatively, one can determine lifetime in the time domain by directly measuring the decay in fluorescence after a pulsed excitation, using time-gated imaging for wide-field FLIM or time-correlated single-photon counting (TCSPC) in point scanning systems.[5]

The diagnostic potential of fluorescence-lifetime-based imaging to distinguish among types or states of tissue was demonstrated previously in a number of *in vitro*, *ex vivo*, and *in vivo* studies (Refs. 5 and 6 and references therein). However, there is a major need to develop practical FLIM instrumentation for *in vivo* applications, for example, to differentiate normal and cancerous tissue. Whereas several endoscopic systems that are capable of single-point time-resolved fluorescence spectroscopy were recently reported,[7–9] there has been little research on endoscopic FLIM systems. For *in vivo* diagnostic applications there is a requirement for high-speed imaging to minimize motion artifacts that precludes scanning TCSPC-based FLIM systems. A frequency-domain endoscopic FLIM instrument has been reported[10] that achieved video-rate FLIM of biological tissue for a limited spatial resolution of 32×32 pixels. In the time domain, a wide-field endoscopic FLIM system has been demonstrated,[11] but it required tens of seconds for data acquisition and processing, making it impractical for clinical imaging. Wide-field FLIM at higher speeds has been achieved, although it has not been applied to endoscopy or to tissue autofluorescence. In the frequency domain, an instrument capable of determining fluorescence-lifetime images at 25 Hz (and of resolving lifetime differences at up to 55 Hz for pixel binning down to 164×123) has been demonstrated.[12] In the time domain, wide-field FLIM has been demonstrated at up to 100 Hz by use of an optical delay line that provided two time-delayed images at a gated optical intensifier (GOI).[13] Although this elegant scheme achieved record FLIM rates, the resultant field of view is halved (from 128×126 pixels) and the optomechanical time delay limits the flexibility to image a wide range of fluorophore lifetimes[14] as well as placing significant size constraints on the system.

We present a full-field, electronically adjustable time-domain instrument that provides FLIM images in real time with a maximum update rate of 29 Hz, which we have applied to multiwell plate imaging and to endoscopy of biological tissue. The system is based on a GOI with a rapidly adjustable electronic delay circuit to permit optimization of the lifetime contrast for different fluorophores. For endoscopic FLIM of tissue autofluorescence we use a compact UV picosecond solid-state laser excitation source (Spectra-Physics, Inc., Model Vanguard 350-HMD355) together with a standard clinical rigid endoscope (Smith & Nephew plc, Model 3894 arthroscope) that provides a wide (~80°) field of view.

Figure 1 shows a schematic of the endoscopic FLIM system. The excitation source was a frequency-tripled diode-pumped mode-locked Nd:YVO_4 laser generating 355-nm wavelength pulses of 10-ps duration at an 80-MHz repetition rate. This compact ultrafast

0146-9592/04/192249-03$15.00/0

UV laser does not require water cooling and is small enough for a 19-in. (48.26-cm) rack-based instrument. The 355-nm radiation will excite many endogenous tissue fluorophores, and the available average power (as much as 350 mW) is typically sufficient to overcome the losses associated with rigid and flexible endoscopes. The fluorescence image of approximately 32 mm × 22 mm at 4.5-cm working distance was acquired with the rigid endoscope and relayed onto the 18-mm-diameter photocathode of a wide-field double microchannel plate GOI (Kentech Instruments, Ltd., Model HRI) via a long-pass glass filter (Schott GG435) to block the reflected excitation light. This GOI is operated at the same repetition rate as the laser (80 MHz), with gate widths adjustable to a minimum of 300 ps. A low-jitter electronic delay generator synchronized to the frame grabber's status signal adjusted the relative delay between time-gated images and was reconfigurable to within 2.5 ms. Time-gated fluorescence images were relayed from the GOI phosphor to a 1344 × 1024 pixel CCD camera (Hamamatsu Model ORCA ER), where on-chip integration was performed. The images were hardware binned four times to increase sensitivity and readout speed. The resultant 336 × 256 pixel images were sufficient to prevent undersampling of the GOI phosphor screen. The final measured spatial resolution of this endoscopic FLIM system was 0.05 mm.

In an approach similar to that described by Agronskaia *et al.*[13] the fluorescence-lifetime maps were calculated by use of a rapid lifetime determination (RLD) algorithm.[15] Assuming single exponential decay profiles, this algorithm requires two time-gated fluorescence images recorded at different delays with respect to the excitation pulse for each lifetime map. The decay parameters were evaluated from the ratio of integrated areas under two different regions of the decay curve. We rendered the resultant FLIM images by mapping each lifetime value to a color scale and subsequently intensity weighting each pixel value. Using speed-optimized code written in C^{++} and running on a 2.8-GHz Pentium 4 processor in Windows XP, we updated the FLIM images and the first time-gated image at a rate determined by the sample fluorescence intensity up to a maximum of 29 Hz, which is the maximum frame rate of the CCD camera. One could achieve higher update rates by reducing the number of pixels in the field of view. If required, one can enhance the apparatus's sensitivity by increasing the CCD integration time and reducing the update rate correspondingly.

To assess the performance of this real-time FLIM instrument, we acquired lifetime maps of a multiwell plate array with different dye solutions, using both the endoscope and a wide-field macroimager, in which the endoscope was replaced by a standard (f/No. 1.8) camera lens. The microwells were alternately filled with 20-μl of a solution of Stilbene 1 in methanol and Coumarin 314 in a solvent mixture of 60% ethanol and 40% glycerol. FLIM maps were obtained by use of the RLD algorithm with two time gates of 1.8-ns duration as described above, at update rates of 29 and 7.2 Hz (such that $\sim 3 \times 10^6$ and 11×10^6 laser pulses at 80 MHz were detected for each FLIM image), and compared with those obtained with a standard weighted nonlinear least-squares (WNLLS) algorithm to fit a monoexponential decay to a series of short (400-ps) time-gated images obtained in ~600 ms. The WNLLS algorithm required ~10 s for data processing to generate a FLIM map.

Figures 2(a) and 2(b) show FLIM maps obtained with the wide-field macroimager with the WNLLS fitting algorithm and the RLD algorithm (with a gate separation of 2.00 ns), respectively, the latter at a video-rate (29-Hz) update rate. These FLIM maps are almost indistinguishable, reporting average Stilbene 1–Coumarin 314 solution lifetimes of 0.93 ± 0.04 ns–3.50 ± 0.24 ns and 0.89 ± 0.03 ns–3.50 ± 0.20 ns for WNLLS and RLD algorithms, respectively. Figures 2(c) and 2(d) show FLIM maps acquired through the endoscope (by external excitation) at update rates of 29 and 7.2 Hz, yielding average lifetime values of 0.90 ± 0.11 ns–3.50 ± 0.83 ns and 0.91 ± 0.09 ns–3.60 ± 0.64 ns, respectively. The reduced light collection efficiency through the endoscope results in a lower signal-to-noise ratio and broader lifetime histograms, as shown in Figs. 2(e) and 2(f), but it does not severely affect the lifetime contrast. The shortest lifetime experimentally determined was 120 ± 10 ps, although we were able to image lifetime differences as small as 80 ps for two similar lifetime dyes. The interval between consecutive excitation laser pulses limits to ~4 ns the longest lifetime that can be optimally determined. Longer lifetimes can be measured with reduced signal-to-noise ratios, which will depend on the sample's fluorescence intensity.[14]

To demonstrate that endoscopic FLIM may be practical for clinical imaging, we applied this instrument *ex vivo* to biological tissue. Figure 3 shows endoscopic fluorescence-lifetime images of a bisected lamb kidney acquired by use of both the standard WNLLS and RLD algorithms (3.00-ns gate separation). Both FLIM images were obtained with the FLIM endoscope system described above, with an incident intensity of 28 mW/cm^2 at the sample. Intrinsic fluorescence-lifetime contrast can be observed among the renal cortex, the medulla, and the calyces, and the renal pelvis.

We note that, although tissue components generally exhibit complex exponential decay profiles and may be more thoroughly analyzed by use of a stretched

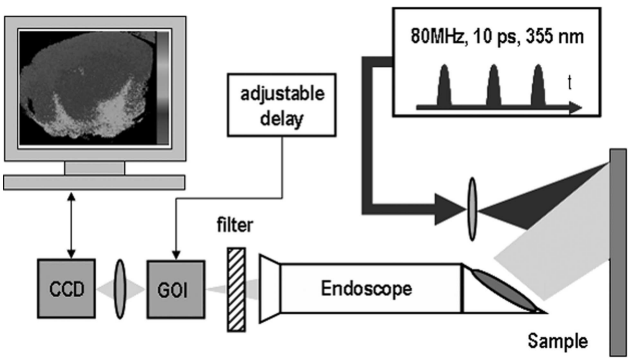

Fig. 1. Experimental setup for the endoscopic FLIM.

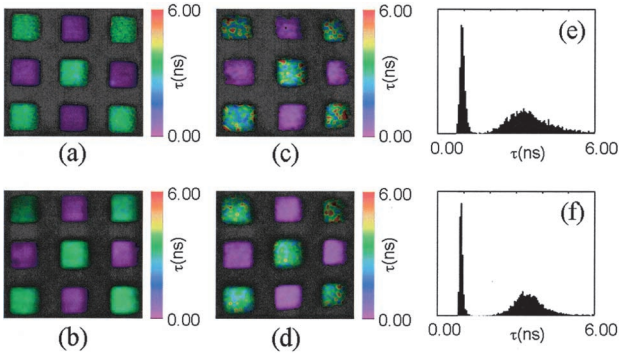

Fig. 2. Intensity weighted fluorescence-lifetime images of a multiwell plate array of alternating solutions of Stilbene 1 and Coumarin 314. (a), (b) Obtained through a wide-field macro-imager by use of the WNLLS fitting algorithm and the RLD algorithm respectively; (c), (d) obtained with the endoscopic FLIM instrument with RLD determination at update rates of 29 and 7.2 Hz, respectively (e), (f) Lifetime histographs that correspond to (c) and (d), respectively.

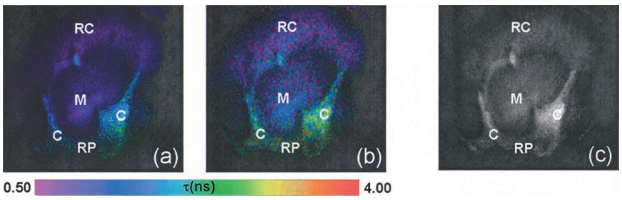

Fig. 3. Endoscopic intensity weighted fluorescence-lifetime images of a bisected lamb kidney, showing lifetime contrast among the renal cortex (RC), the medulla (M), the renal pelvis (RP), and the calyces (C). (a) Obtained with the WLLNS algorithm with eight time-gated images of 400-ps duration and required 15 s for data acquisition and processing; (b) obtained with the RLD algorithm by use of only two gates of 1.0 ns each at an update rate of 7.2 Hz. (c) Integrated fluorescence intensity imaging that corresponds to (a).

exponential function,[16] the single exponential fit provides a useful approximation that still yields physiological contrast. As this system can image lifetime differences of less than 100 ps, it can be adequate for contrasting healthy and malignant tissues, e.g. Ref. 6. Even though the signal-to-noise ratio of the FLIM map computed with the standard WLLNS algorithm is higher than that of the FLIM map obtained with the RLD algorithm, updating the former required ~15 s, a time that is incompatible with clinical requirements, whereas the latter provided a real-time FLIM image with an update rate of 7.2 Hz. One could obtain improved lifetime discrimination by adapting the RLD algorithm to use more time gates at the expense of a lower FLIM imaging rate; with the current electronically controlled delay line and acquisition system, doing so could still yield real-time information. In a more-sophisticated instrument, one could envisage a RLD FLIM mode's being used to help a clinician to search for specific features or abnormalities by use of a higher-precision, slower frame rate mode that uses more time-gated images for more-detailed analysis of complex fluorescence contrast at a specific location.

In conclusion, we have demonstrated a high-speed wide-field time-domain FLIM instrument that provides fluorescence-lifetime images in real time, including through an endoscope. The FLIM data acquisition is entirely electronically controlled and may be rapidly adjusted to suit a wide range of fluorophore lifetimes. Using a compact UV mode-locked-laser excitation source, we have demonstrated *ex vivo* endoscopic FLIM of biological tissue, showing that this approach can provide useful intrinsic contrast at practical frame rates for clinical diagnosis and other applications. This high-speed FLIM technology may also be applied to wide-field microscopy of dynamic samples, e.g., for calcium imaging or motion analysis, and to high-throughput assays.

This research was funded by a Beacon award from the Department of Trade and Industry, UK, and a Showcase award from The Wellcome Trust. We thank Smith & Nephew plc for donating the endoscope. J. Requejo-Isidro's e-mail address is j.requejo@imperial.ac.uk.

References

1. R. A. Drezek, R. Richards-Kortum, M. A. Brewer, M. S. Feld, C. Pitris, A. Ferenczy, M. L. Faupel, and M. Follen, Cancer **98,** 2015 (2003).
2. J. R. Lakowicz, *Principles of Fluorescence Spectroscopy*, 2nd ed. (Plenum, New York, 1999).
3. K. Dowling, M. J. Dayel, M. J. Lever, P. M. W. French, J. D. Hares, and A. K. L. Dymoke-Bradshaw, Opt. Lett. **23,** 810 (1998).
4. T. W. J. Gadella, T. M. Jovin, and R. M. Clegg, Biophys. Chem. **48,** 221 (1993).
5. R. Cubeddu, D. Comelli, C. D'Andrea, P. Taroni, and G. Valentini, J. Phys. D **35,** R61 (2002).
6. P. J. Tadrous, J. Siegel, P. M. W. French, S. Shousha, E.-N. Lalani, and G. W. H. Stamp, J. Pathol. **199,** 309 (2003).
7. Q. Fang, T. Papaioannou, J. A. Jo, R. Vaitha, K. Shastry, and L. Marcu, Rev. Sci. Instrum. **75,** 151 (2004).
8. J. D. Pitts and M.-A. Mycek, Rev. Sci. Instrum. **72,** 3061 (2001).
9. T. Glanzmann, J.-P, Ballini, H. van den Bergh, and G. Wagnières, Rev. Sci. Instrum. **70,** 4067 (1999).
10. J. Mizeret, T. Stepinac, M. Hansroul, A. Studzinski, H. van den Bergh, and G. Wagnières, Rev. Sci. Instrum. **70,** 4689 (1999).
11. J. Siegel, D. S. Elson, S. E. D. Webb, K. C. Benny Lee, A. Vlandas, G. L. Gambaruto, S. Lévêque-Fort, M. J. Lever, P. J. Tadrous, G. W. H. Stamp, A. L. Wallace, A. Sandison, T. F. Watson, P. M. W. French, and F. Alvarez, Appl. Opt. **42,** 2995 (2003).
12. O. Holub, M. J. Seufferheld, C. Gohlke, Govindjee, and R. M. Clegg, Photosynthetica **38,** 581 (2000).
13. A. V. Agronskaia, L. Tertoolen, and H. C. Gerritsen, J. Phys. D **36,** 1655 (2003).
14. R. M. Ballew and J. N. Demas, Anal. Chem. **61,** 30 (1989).
15. X. F. Wang, T. Uchida, D. M. Coleman, and S. Minami, Appl. Spectrosc. **45,** 360 (1991).
16. K. C. Benny Lee, J. Siegel, S. E. D. Webb, S. Lévêque-Fort, M. J. Cole, R. Jones, K. Dowling, M. J. Lever, and P. M. W. French, Biophys. J. **81,** 1265 (2001).